

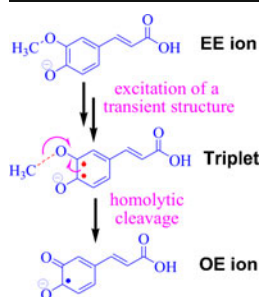
# On the Origin of the Methyl Radical Loss from Deprotonated Ferulic and Isoferulic Acids: Electronic Excitation of a Transient Structure

Xiaoping Zhang,<sup>1,2</sup> Fei Li,<sup>1</sup> Huiqing Lv,<sup>3</sup> Yanqing Wu,<sup>1</sup> Gaofeng Bian,<sup>1</sup> Kezhi Jiang<sup>1</sup>

<sup>1</sup>Key Laboratory of Organosilicon Chemistry and Material Technology, Hangzhou Normal University, Hangzhou 310012, China

<sup>2</sup>College of Chemical Engineering and Material Science, Zhejiang University of Technology, Hangzhou 310014, China

<sup>3</sup>College of Pharmaceutical Sciences, Zhejiang Chinese Medical University, Hangzhou, Zhejiang 310053, China



**Abstract.** Formation of radical fragments from even-electron ions is an exception to the “even-electron rule”. In this work, ferulic acid (FA) and isoferulic acid (IFA) were used as the model compounds to probe the fragmentation mechanisms and the isomeric effects on homolytic cleavage. Elimination of methyl radical and CO<sub>2</sub> are the two competing reactions observed in the CID-MS of [FA – H]<sup>–</sup> and [IFA – H]<sup>–</sup>, of which losing methyl radical violates the “even-electron rule”. The relative intensity of their product ions is significantly different, and thereby the two isomeric compounds can be differentiated by tandem MS. Theoretical calculations indicate that both the singlet-triplet gap and the excitation energy decrease in the transient structures, as the breaking C–O bond is lengthened. The methyl radical elimination has been

rationalized as the intramolecular electronic excitation of a transient structure with an elongating C–O bond. The potential energy diagrams, completed by the addition of the energy barrier of the radical elimination, have provided a reasonable explanation of the different CID-MS behaviors of [FA – H]<sup>–</sup> and [IFA – H]<sup>–</sup>.

**Key words:** Methyl radical elimination, Ferulic acid, Isoferulic acid, Electronic excitation, Transient structure, Isomeric differentiation

Received: 21 December 2012/Revised: 28 January 2013/Accepted: 5 February 2013/Published online: 12 April 2013

## Introduction

The combination of electrospray ionization (ESI) mass spectrometry with collision-induced dissociation (CID) technique is an indispensable analytical tool, which has been widely used to analyze a large variety of organic and pharmacologic compounds [1–3]. Successful structure elucidation based on tandem mass spectrometry (MS/MS) data is dependent on correct interpretation of the fragmentation pathways. The ions generated in the electrospray process are predominantly stable ionic species with closed-shell electronic structures, such as [M + H]<sup>+</sup>, [M + Na]<sup>+</sup>, and [M – H]<sup>–</sup>. Upon low energy collisional activation, dissociation of the closed-shell ions usually follows the “even-electron rule” [4], and leads to closed-shell fragment ions and neutral fragments [5, 6].

Over the years, several reports have appeared in the literature describing violations of the “even-electron rule”, in which an ESI-generated closed-shell ion dissociates to give an odd-electronic (OE) ion [7–19]. It is desirable and significant to investigate the underlying mechanism on the formation of OE ions from even-electronic (EE) ions because such considerations are important for better structural elucidation by ESI tandem mass spectrometry.

Most of the violations occur in cases that involve aromatic, resonance-stabilized radicals as fragmentation products [9–13], indicating that they also obey thermodynamic rules [4]. Thus, the resonance stabilization renders the spin forbidden decomposition channel accessible. It was also proposed that aromatic stabilization leads to lower energy barriers, which might kinetically favor the generation of the radical fragments [4]. Sometimes, when the competing decomposition channels are not available, radical species appear as the fragment products [12].

A single electron transfer (SET) mechanism via the electron excitation in an ion/neutral complex (INC), which results from the heterolytic cleavage of the EE precursor ions driven by the positive charge, was proposed to be the key

**Electronic supplementary material** The online version of this article (doi:10.1007/s13361-013-0604-2) contains supplementary material, which is available to authorized users.

Correspondence to: Kezhi Jiang; e-mail: jiangkezhi@hznu.edu.cn

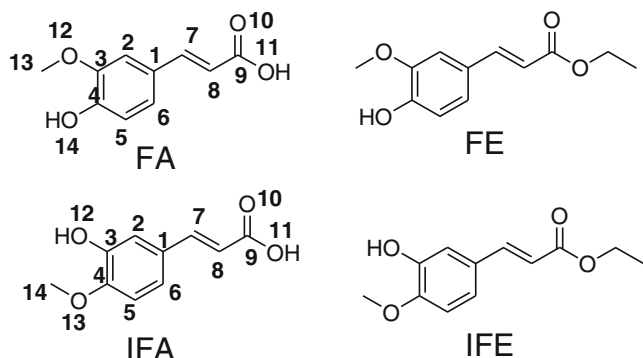
step in the OE ions formation from the dissociation of some protonated molecules, rather than the simple homolytic bond cleavage [14–16]. Formation of radicals from the homolytic cleavage of the precursor ion may also occur with the involvement of an electronically excited state. Hau et al. described the radical elimination of closed shell pyridinium cations with the involvement of a cation diradical [17]. Although not specified by the authors, such an intermediate may correspond to a triplet state. Theoretical calculations show that the singlet-triplet gap for transient structures with an elongated benzylic C–C bond is very low for protonated and alkylated pyridinium cations and radical formation may result from the mixing of these states [18]. Recently, Cabrera et al. proposed that dissociation of the lowest triplet excited state would provide a reasonable interpretation for the radical loss of the protonated hydroxypyridine N-oxides [19]. However, the fragmentation mechanisms for the homolytic cleavage processes have not been well documented, especially for the radical elimination of anions [11].

Many natural products, such as methoxyl phenolic compounds [20], flavonoid *O*-glycosides [3, 21], and oxygenated tetracyclic triterpenoids [22], have reported to form radical anions in the negative tandem MS. Ferulic acid (FA) and isoferulic acid (IFA) are phenolic plant metabolite compounds, that exhibits antioxidative properties and a large variety of therapeutic effects against various diseases [23–25]. In the present work, we demonstrate a special case where the methyl radical expulsion competes with the CO<sub>2</sub> elimination upon low-energy dissociation of the deprotonated FA and IFA molecules in the negative ESI tandem mass spectrometry. Experimental and theoretical approaches are employed to investigate the mechanisms of this decomposition and the isomeric effect.

## Experimental

### Chemicals

FA and IFA (purity 99.0 %, Scheme 1) were purchased from Sigma-Aldrich (Milwaukee, WI, USA). Ethyl ferulate (FE) and ethyl isoferulate (IFE) were synthesized by the reaction



Scheme 1. Structures of ferulic acid, isoferulic acid, and their ethyl and benzyl esters

and ethyl isoferulate (IFE) were synthesized by the reaction of the corresponding acid with ethanol in the presence of SOCl<sub>2</sub>, and identified by IR, MS, and NMR.

Methanol (HPLC grade) was obtained from Merck (Darmstadt, Germany). Purified water was prepared by using Milli-Q water purification system (Millipore, Bedford, USA).

### Mass Spectrometry

The MS/MS experiments were performed on a microTOF QII (Q-TOF) mass spectrometer from Bruker Daltonics (Billerica, MA, USA), equipped with an ESI ion source. The diluted solvent was directly infused into the electrospray ionization source of the mass spectrometer with a syringe pump at a flow rate of 180 μL/h. The parameters of Q-TOF mass spectrometers were set as follows: drying gas flow in the ion source was set up to 4 L/h and nebulizer gas pressure to 0.4 × 10<sup>5</sup> Pa (both were N<sub>2</sub>), the temperature of ion source was 180 °C, and voltage was –3.5 kV. In MS/MS experiments, mass width of the selected ion was 6 Da, and the collision energy of CID for the selected ions was set at the range of 3 to 15 eV with Argon as the collision gas. The instrument was operated at a resolution higher than 15,000 full width at half maximum using the microTOF-Q control program ver. 2.3. The data were analyzed using the Data Analysis ver. 4 software package delivered by Bruker Daltonics.

### Theoretical Calculation

The theoretical calculations were performed using the Gaussian 03 program [26]. The equilibrium geometries of the target species were optimized using the density functional theory (DFT) method at the B3LYP/6-311+G(2d, p) level. The optimized structures were identified as the true minima in energy by the absence of imaginary frequencies. Vibrational frequencies and zero-point energies (ZPE) for all the key species were calculated at the same level of theory. The electron excitation energy of a transient structure was obtained by the Configuration Interaction approach (CI-Singles). The optimized structures were displayed by the Gauss View (Version 3.09) software. Hard data on geometries of all structures involved are available as Supporting Information. The energies discussed here are the sum of electronic and thermal free energy.

## Results and Discussion

### CID Behavior

*Fragmentation of the Deprotonated Ferulic Acid* Figure 1a gives the CID mass spectrum of the deprotonated FA ([FA – H]<sup>–</sup>, *m/z* 193) obtained with a Q-TOF mass spectrometer, and the accurate MS/MS results are summarized in Table 1S in the Supporting Information. Decomposition of [FA – H]<sup>–</sup> mainly generates three fragment ions at *m/z* 178, 149, and

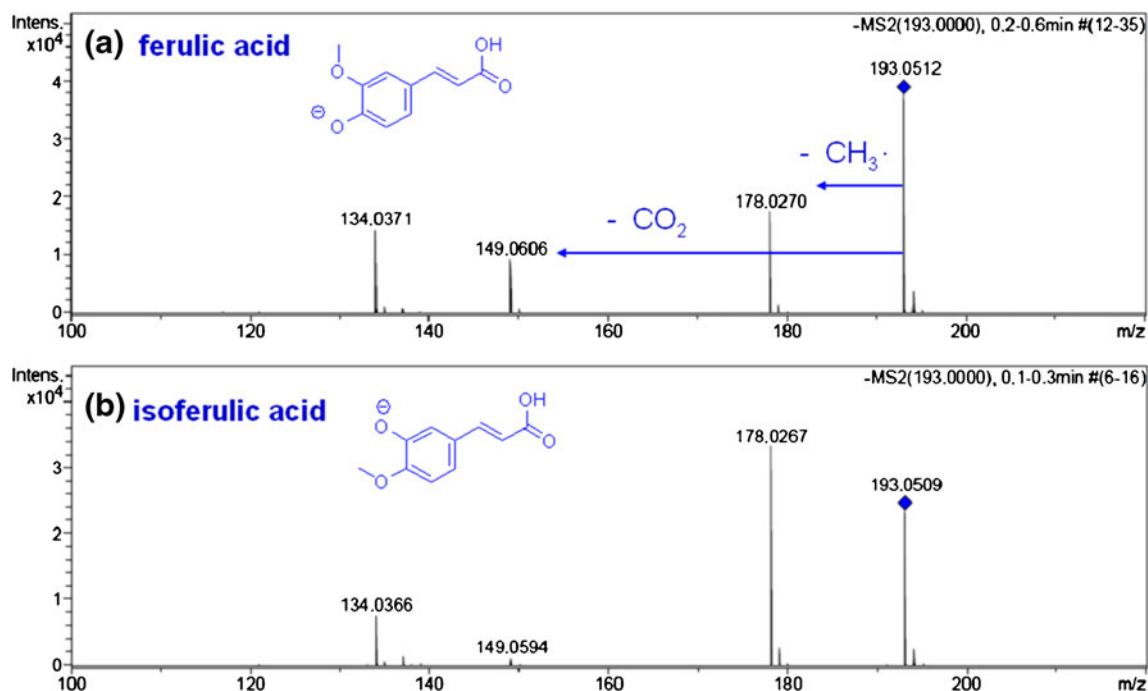


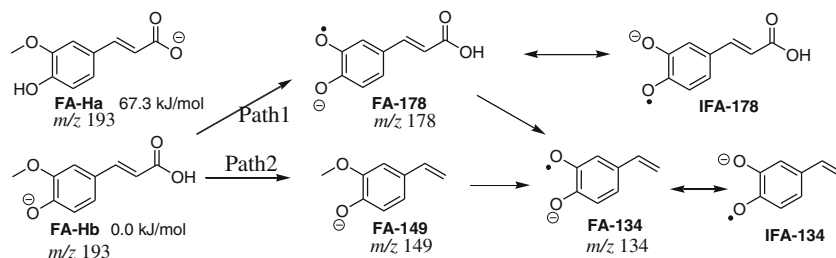
**Figure 1.** Tandem mass spectrometry of the deprotonated ferulic acid (a) and the deprotonated isoferulic acid (b) by ESI-Q/TOF with the collision energy at 8 eV

134, and the reaction pathways are given in Scheme 2. The basic fragment ion at  $m/z$  178 is identified as the deprotonated 3-(3,4-dihydroxy phenyl)acrylic acid radical according to the “nitrogen rule”, which resulted from the methyl radical elimination of the precursor ion  $m/z$  193. Methyl radical loss is a shared feature of methoxyl-substituted aromatic compounds [20]. The fragment ion  $m/z$  149 is attributed to the 2-methoxy-5-vinyl phenolate anion, originating from the  $\text{CO}_2$  elimination of the precursor ion. The fragment ion  $m/z$  134 is also a radical anion, the deprotonated 4-vinylbenzene-1,2-diol radical, resulting either from the  $\text{CO}_2$  elimination of the fragment ion  $m/z$  178 or from the methyl radical elimination of the ion  $m/z$  149. The formulas of these proposed fragment ions are supported by accurate mass measurements obtained by ESI-Q-TOF, in which the relative errors between the measured and the calculated masses for the assigned structures are less than 5 ppm for all the abundant ions in Table 1S in the Supporting Information. Herein, the fragment ions at  $m/z$

178 and 134 are more attractive because they are radical anions with the electron open-shell structure and their formation involves the violation of the “even-electron rule” [4–7]. The fragmentation mechanisms and the isomeric effects for the radical elimination will be documented in detail in the following work.

*The Effect of the Substitution Pattern* To probe the effect of the substituent pattern on the formation of the radical anions, fragmentation of the deprotonated IFA,  $[\text{IFA} - \text{H}]^-$ , has also been investigated to compare the fragmentation behavior of  $[\text{FA} - \text{H}]^-$  (Figure 1). As expected,  $[\text{IFA} - \text{H}]^-$  displays similar reaction channels to  $[\text{FA} - \text{H}]^-$  in the CID process, which leads to the corresponding product ions at  $m/z$  178, 149, and 134 (Scheme 1S in the Supporting Information).

Interestingly, the relative intensity of these product ions is significantly different between the two isomers under the same CID conditions, indicating that the two isomeric compounds can be differentiated by tandem MS. The



**Scheme 2.** The proposed fragmentation channels for FA-Hb

precursor ion ( $m/z$  193) of  $[\text{FA} - \text{H}]^-$  is the base peak, and its fragment ion  $m/z$  178 has a relative intensity of 46.7 % (Table 1S in the Supporting Information). In contrast, the fragment ion  $m/z$  178 rather than the precursor ion becomes the base peak in the MS/MS spectrum for  $[\text{IFA} - \text{H}]^-$ , and the relative intensity of the precursor ion reduces to 71.2 %. Furthermore, the fragment ion  $m/z$  149 originating from the  $\text{CO}_2$  elimination of  $[\text{FA} - \text{H}]^-$  is significantly more abundant than the corresponding fragment ion from  $[\text{IFA} - \text{H}]^-$  (24.6 % in FA versus 3.4 % in IFA).

To gain more insight into these different fragmentation behaviors, CID product ion mass spectra of  $[\text{FA} - \text{H}]^-$  and  $[\text{IFA} - \text{H}]^-$  have been acquired with various collision energies ranging from 3 to 15 eV [11]. Breakdown curves have been plotted in Figure 2, and show the relationship between the relative abundance of selected ions and the collision energy. It is apparent that both  $[\text{FA} - \text{H}]^-$  and  $[\text{IFA} - \text{H}]^-$  undergo decomposition to the first product ions at  $m/z$  178 and 149, and that the secondary product ion  $m/z$  134 is formed from the ion at  $m/z$  178 or 149. Decomposition of  $[\text{IFA} - \text{H}]^-$  is more facile than that of  $[\text{FA} - \text{H}]^-$  at various collision energies, which mainly leads to the open-shell product ion at  $m/z$  178. For the competing reactions leading to the first product ions,  $\text{CO}_2$  elimination of  $[\text{FA} - \text{H}]^-$  is significantly more facile than that of  $[\text{IFA} - \text{H}]^-$ .

**The Effect of Esterification** To gain more insight into the effect of the chemical structure on the homolytic cleavage of the EE ions, ethyl ferulate (FE) and ethyl isoferulate (IFE) have been synthesized for the negative tandem MS investigation. For the occurrence of FE and IFE, the carboxyl group has been protected by ethyl esterification, which will prevent the competing dissoci-

ation channel of losing  $\text{CO}_2$ . As expected, only the radical species at  $m/z$  206, resulting from the methyl radical elimination of  $[\text{FE} - \text{H}]^-$  or  $[\text{IFE} - \text{H}]^-$ , has been observed in the CID mass spectra (Figure 1S in the Supporting Information). Identification of the radical fragments has also been substantiated by the accurate mass spectral data (Table 1S in the Supporting Information). Similar to FA and IFA,  $[\text{IFE} - \text{H}]^-$  is somewhat more facile towards methyl radical elimination than  $[\text{FE} - \text{H}]^-$ .

### Computational Study

According to the above experimental results, two reaction channels have been proposed for the dissociation of  $[\text{FA} - \text{H}]^-$  and  $[\text{IFA} - \text{H}]^-$ . Path-1 involves methyl radical elimination prior to  $\text{CO}_2$  decomposition, whereas  $\text{CO}_2$  decomposition is followed by methyl radical elimination in Path-2 (Scheme 2 and Scheme 1S). The fragmentation channels of  $[\text{FA} - \text{H}]^-$  and  $[\text{IFA} - \text{H}]^-$  have been investigated by DFT theoretical calculations at the uB3LYP/6-311+G(2d,p) level to probe the fragmentation reactions.

**Deprotonation Site** FA has two active protons in its structure, the carboxylic proton H11 and the phenolic hydroxyl proton H14 (Scheme 1), and each has the potential to undergo deprotonation during the negative ESI process, and give FA-Ha and FA-Hb, respectively. The deprotonation site was reported to be affected largely by the solvent used in the ESI process under the conditions that trace (mM) KOH or LiOH was added in to the ESI solvent [27, 28]. In the absence of KOH or LiOH, however, the MS/MS spectra

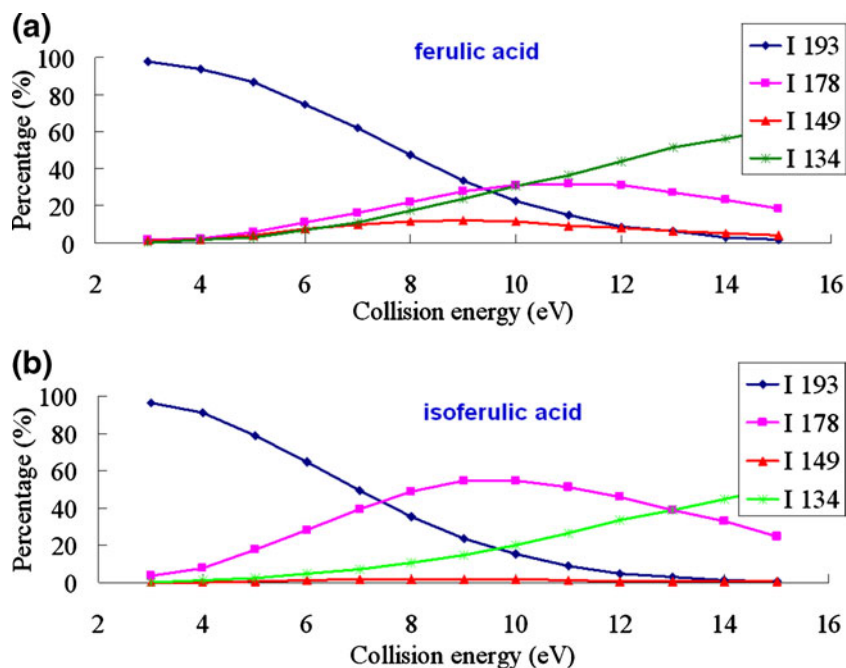


Figure 2. The energy-resolved plot for  $[\text{FA} - \text{H}]^-$  (a) and  $[\text{IFA} - \text{H}]^-$  (b)

of  $[FA - H]^-$  are practically identical irrespective whether methanol or acetonitrile is used in the electrospray process, while the MS/MS spectrum varies distinctively in the presence of KOH (Figure 2S in the Supporting Information). Therefore, deprotonation of the neutral molecule of FA in the ESI process is hardly affected by the ESI solvent.

The calculated free energy of FA–Ha is 67.3 kJ/mol higher than that of FA–Hb, indicating that the phenolic hydroxyl proton is more likely to undergo dissociation in the ESI process than the carboxylic proton. The stability of FA–Hb results from the resonance effect, which disperses the negative charge onto the phenyl group and the allyl acetic moiety (Scheme 3); the negative charge in FA–Ha is mainly localized on the carboxylic group. Thus, deprotonation of FA primarily generates the gas-phase FA–Hb in the negative ESI process due to the remarkable energetic difference between FA–Ha and FA–Hb.

Similar to FA, the phenolic hydroxyl group of IFA is also thermodynamically more favorable to undergo deprotonation than the carboxylic group does in the gas phase because of the resonance stabilization (Scheme 3). However, the negative charge in IFA-b cannot be dispersed onto the allyl acetic moiety, because of the *meta* position of the phenolic hydroxyl anion. As a result, IFA-b lies 32.9 kJ/mol above FA-b in free energy, indicating that fragmentation of the deprotonated IFA is more favorable than FA, which is in agreement with the CID MS results.

**Mechanistic Investigation of the Radical Elimination** The radical elimination pathway of FA–Hb has been characterized by stepwise increase in the length of the breaking methoxyl C–O bond, while optimizing all other coordinates at each given bond length. The curve with dots in Figure 3 describes the potential energy curve for the disruption of the methoxyl O–C bond in FA–Hb (the singlet state) calculated at the uB3LYP/6-31g(d) level. For a typical reaction, it is straightforward to optimize the transition state geometry from the point with the highest energy along the path. However, the energy of FA–Hb increases monotonically as the O–C bond is elongated. The

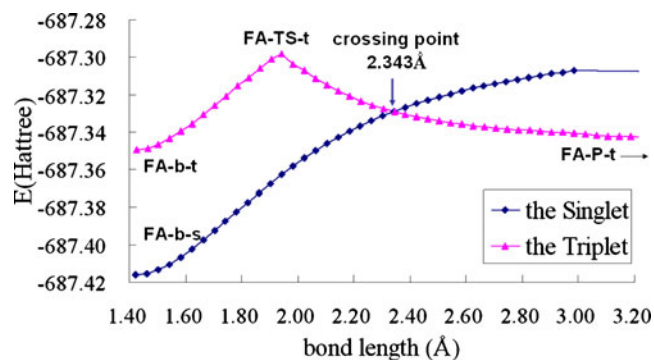
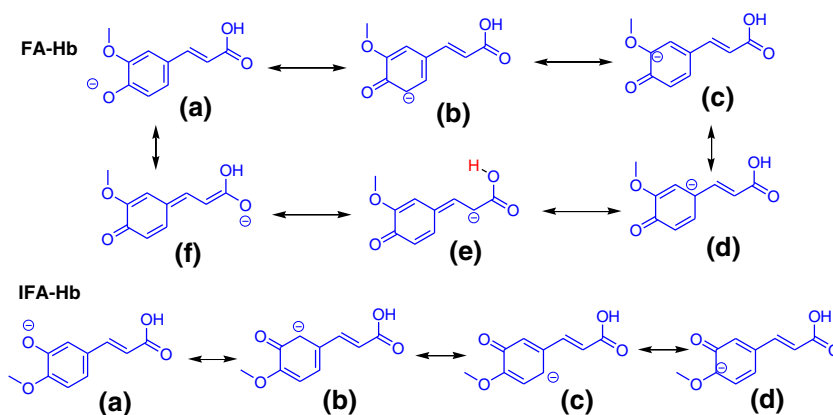


**Figure 3.** Calculated potential energy curves for the radical fragmentation of the singlet (dots) and the triplet (triangles) FA–Hb

calculated transition state (TS) may represent a plateau in the fragmentation channel rather than a saddle point. DFT methods often fail to locate a transition state along the reaction coordinates in the homolytic reactions, due to difficulties in treating the self-interaction of electrons [12, 18, 19, 29]. This leads to inaccurate estimation of TS energies for the radical loss process. The calculated considerable TS value (247.8 kJ/mol) obviously disagrees with the highly efficient homolytic cleavage observed in the CID-MS experiments, and distinctively overestimates the actual energy barrier in the radical elimination of FA–Hb.

Radical formation from closed-shell ions has been reported to occur via the involvement of an electronically excited state, such as the triplet state [17–19]. A full geometry optimization and frequency analysis have been carried out for the singlet and the triplet states of FA–Hb. Both have near planar geometries (Figure 3S in the Supporting Information), but the triplet one (FA–Hb–t) has longer ring bond lengths than the singlet state (FA–Hb), indicating that FA–Hb–t is formed by excitation of a  $\pi$  electron of the phenyl ring into the *anti*  $\pi$  orbital. Moreover, natural bond orbital (NBO) analysis of FA–Hb shows that the HOMO (51) and LUMO (52) of FA–Hb are all mainly located at the phenyl ring (Figure 4). The radical center at the phenyl



**Scheme 3.** The resonance of FA–Hb and IFA–Hb

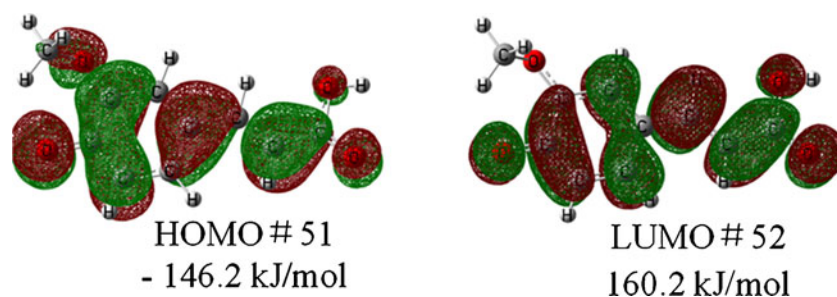


Figure 4. HOMO and LUMO of FA-Hb

ring will initiate the disruption ( $\alpha$  cleavage) of the neighboring C–O bond in the methyl radical elimination of the FA-Hb-t.

As shown in Figure 3, there is a maximum, FA-TS-t, in the potential energy curve (with triangles) for scanning the methoxyl C–O bond distance in FA-Hb-t. DFT calculations indicate that FA-TS-t lies 105.2 kJ/mol above FA-Hb-t in free energy. Therefore, the overall energy barrier via FA-TS-t is 270.3 kJ/mol relative to the initial FA-Hb geometry, since FA-Hb-t is located at 164.9 kJ/mol above the singlet FA-Hb. Such a considerable energy barrier seriously inhibits the occurrence of the reaction channel, in which excitation occurs prior to homolytic cleavage.

Nevertheless, the calculated vertical singlet-triplet transition energies decrease as the O–C bond is lengthened, as shown in Figure 3. The calculated PES scans of the singlet ground state and the triplet excited state cross at a certain point, at which the electronic excitation is a thermodynamically favorable process. The crossing point corresponds to a transient structure of FA-Hb with the C–O bond length of approximately 2.343 Å. Because electron excitation occurs on the femtosecond ( $10^{-15}$ s) times scale, while the vibrational motion occurs on the 100 femtosecond ( $10^{-13}$ s) time scale, electronic excitation is well likely to perform for a transient structure of FA-Hb. It is noteworthy that the first excitation energy of the transient structures of FA-Hb decreases gradually as the O–C bond length increases, and that it decreases rapidly when the O–C bond extends beyond 2.0 Å (Figure 5). The first excitation energy drops to 0 eV at a C–O bond length of approximately 2.25 Å, and it is  $-0.78$  eV for the transient structure at the

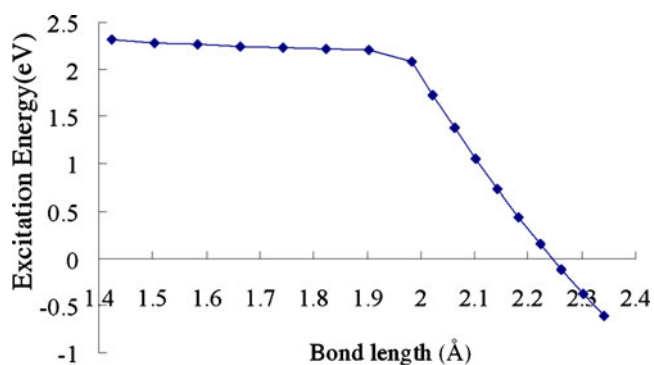


Figure 5. Plot of the first excitation energy and the O–C bond length for the transient structures of FA-Hb

crossing point, indicating a spontaneous electronic excitation process. In addition, there is no significant difference in the structural geometry between FA-Hb and FA-Hb-t at the crossing point. Therefore, the radical elimination channel of FA-Hb can be considered to proceed in the following process: (1) elongation of the O–C bond to approximately 2.343 Å, (2) spontaneous electronic excitation, and (3) subsequent disruption of the O–C bond. The transient structure of FA-Hb at the crossing point can be regarded as the transition state in the methyl radical loss process, with a calculated energy barrier of 203.3 kJ/mol.

Similarly, the PES scans of the singlet and the triplet state of IFA-Hb also cross at a certain point, corresponding to a C–O bond length of approximately 2.263 Å (Figure 4S in the Supporting Information). Frequency analysis of the transient structure of IFA-Hb at the crossing point indicates the transient structure is located at 180.7 kJ/mol above the singlet IFA-Hb in free energy. Similar results have been obtained in investigation of the radical elimination of the other closed shell anions. Therefore, the radical elimination can be rationalized as the electronic excitation of a transient structure, and thus the energy barrier of the radical elimination can be estimated coarsely.

**Dissociation Pathways** In Figure 6, we present a schematic potential energy diagram for the fragmentation reactions of the deprotonated FA. The energy barrier has been estimated to be 203.3 kJ/mol for the methyl radical loss of FA-Hb in Path-1, which is much more favorable than the direct

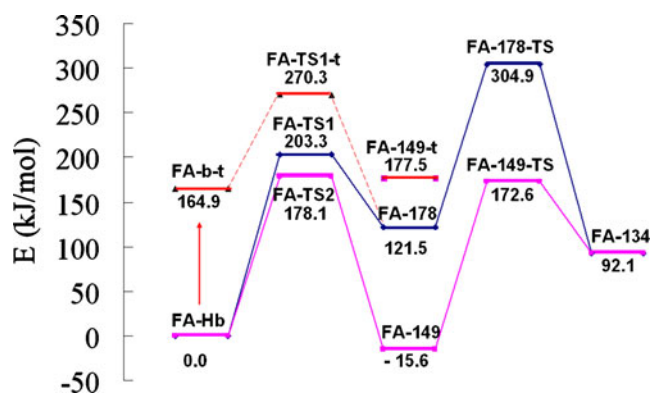


Figure 6. The energy profile of fragmentation of FA-Hb

homolytic cleavage of the triplet state via FA-TS1-t (270.3 kJ/mol). As for the resulting fragment ion FA-178, the radical center is stabilized by aromatic resonance, in which the unpaired electron is delocalized over the whole molecular structure (Table 2S in the Supporting Information). The sum free energy of FA-178 and methyl radical is 121.5 kJ/mol more than that of the precursor ion. However, the subsequent dissociation of FA-178 needs to surmount a considerable energy barrier (304.9 kJ/mol), which greatly restrains the occurrence of the reaction.

For Path-2, FA-Hb first undergoes CO<sub>2</sub> elimination via a four-membered ring transition state FA-TS2, which results in the formation of the fragment ion FA-149 (*m/z* 149). To accomplish this decomposition, rotation of the carboxyl group is essential for migration of the carboxyl hydrogen to the allyl C8, as supported by the dihedral angle  $\Phi$  C7-C8-C9-O11 of 106.4° in FA-TS2. This process is exoergic by 15.6 kJ/mol, and the energy barrier is 178.1 kJ/mol relative to FA-Hb, which is 25.2 kJ/mol lower than the barrier in Path-1. The generated FA-149 then undergoes the methyl radical elimination to yield the open-shell anion FA-134 at *m/z* 134. The energy barrier was assessed to be 172.6 kJ/mol by frequency analysis of the transient structure of FA-134 at the crossing point, originating from the PES scans of its singlet and triplet states (Figure 5S in the Supporting Information).

Comparison of the potential energy diagram of the two reaction channels (Figure 6) indicates that the methyl radical expulsion in Path-1 is kinetically and thermodynamically less favorable than the CO<sub>2</sub> elimination in Path-2. Nevertheless, the formed fragment ion at *m/z* 149 in Path-2 is much facile to undergo further dissociation, because the energy barrier in the second step is less than that in the first one. As a result, abundant fragment ion at *m/z* 134 can be obtained in the CID-MS spectrum, and the fragment ion *m/z* 178 becomes more abundant than the ion *m/z* 149, which is in a good agreement with the tandem MS results (Figure 1a), and is further validated by the breakdown curve in Figure 2.

As for IFA-Hb, the calculated energy barrier for the methyl radical elimination via IFA-TS1 is 180.7 kJ/mol relative to IFA-Hb, which is kinetically more favorable than that of FA-Hb by 19.6 kJ/mol (Figure 6S in the Supporting Information). In addition, the calculated energy of IFA-Hb is 32.9 kJ/mol higher than that of FA-Hb, while their fragment ions, IFA-178 and FA-178, are different resonance forms of the same radical anion. As a result, it is also thermodynamically more favorable for IFA-Hb to undergo the methyl radical elimination than FA-Hb, which also agrees with the tandem MS results.

As shown in Scheme 3, the C8 atom in FA-Hb possesses more negative charge than IFA-Hb because of the resonance effects, and thus FA-Hb is more facile to accept the transferring proton from the carboxylic group during CO<sub>2</sub> elimination. As a result, the CO<sub>2</sub> elimination of IFA-Hb needs to surmount an energy barrier of 202.4 kJ/mol, which is kinetically less favorable than that of FA-Hb by 24.3 kJ/mol. In contrast, the resulting IFA-149 needs only to surmount an

energy barrier of 143.8 kJ/mol to undergo the methyl radical elimination, according to the frequency analysis of the transient structure at the crossing point of the PES scans of the singlet and triplet states (Figure 7S in the Supporting Information). As a result, the fragment ion IFA-149 has a low intensity, because it can readily undergo further fragmentation when it is formed. In conclusion, these potential energy diagrams, completed by the addition of the energetic barrier for the radical elimination, have helped to provide a reasonable explanation of the different CID-MS behaviors for these isomeric species.

## Conclusion

The fragmentation of deprotonated ferulic and isoferulic acids has been investigated experimentally and theoretically. Losses of methyl radical and CO<sub>2</sub> are the two main fragmentation pathways for [FA-H]<sup>-</sup> and [IFA-H]<sup>-</sup>, in which the methyl radical elimination violates the “even-electron rule”. The mechanism for the methyl radical elimination was proposed to involve the electronic excitation of a transient structure. Thus, the energy barriers can be estimated coarsely by frequent analysis of the transient structure, obtained from the PES scan of the singlet ground state and triplet excited states of the precursor ion. The calculated potential energy diagrams for the fragmentation of [FA-H]<sup>-</sup> and [IFA-H]<sup>-</sup> have helped us rationalize their different CID-MS behaviors of the two isomers. The results presented in this work will provide a better understanding of the radical elimination in CID MS spectra. Further work will be carried out to test this mechanism.

## Acknowledgments

The authors gratefully acknowledge financial support from the National Science Foundation of China (No.21205025) and the National Science Foundation of Zhejiang Province (Y4100020 and Y4110243). Computer time was made available on the SGI Aktix 450 sever at Computational Center for Molecular Design of Organosilicon Compounds, Hangzhou Normal University.

## References

1. Hopfgartner, G., Bourgoigne, E.: Quantitative high-throughput analysis of drugs in biological matrices by mass spectrometry. *Mass Spectrom. Rev.* **22**, 195–214 (2003)
2. Fang, A.S., Miao, X., Tidswell, P.W., Towle, M.H., Goetzinger, W.K., Kyranos, J.N.: Mass spectrometry analysis of new chemical entities for pharmaceutical discovery. *Mass Spectrom. Rev.* **27**, 20–34 (2008)
3. Vukics, V., Guttman, A.: Structural characterization of flavonoid glycosides by multi-stage mass spectrometry. *Mass Spectrom. Rev.* **29**, 1–16 (2010)
4. Karni, M., Mandelbaum, A.: The even-electron rule. *Org. Mass Spectrom.* **15**, 53–64 (1980)
5. McLafferty, F.W., Turecek, F.: Interpretation of Mass Spectra, 4th edn. University Science Books, Mill Valley, CA (1993)
6. Gross, J.H.: Mass Spectrometry: A Textbook. Springer-Verlag, Heidelberg, Germany (2004)

- Thurman, E.M., Ferrer, I., Pozo, O.J., Sancho, J.V., Hernandez, F.: The even-electron rule in electrospray mass spectra of pesticides. *Rapid Commun. Mass Spectrom.* **21**, 3855–3868 (2007)
- Williams, J.P., Nibbering, N.M.M., Green, B.N., Patel, V.J., Scrivens, J.H.: Collision-induced fragmentation pathways including odd-electron ion formation from desorption electrospray ionization generated protonated and deprotonated drugs derived from tandem accurate mass spectrometry. *J. Mass Spectrom.* **41**, 1277–1286 (2006)
- Levsen, K., Schiebel, H.-M., Terlouw, J.K., Jobst, K.J., Elend, M., Preiß, A., Thiele, H., Ingendoh, A.: Even-electron ions: A systematic study of the neutral species lost in the dissociation of quasimolecular ions. *J. Mass Spectrom.* **42**, 1024–1044 (2007)
- Vessecchi, R., Carollo, C.A., Lopes, J.N.C., Crotti, A.E.M., Lopes, N.P., Galembeck, S.E.: Gas-phase dissociation of 1,4-naphthoquinone derivative anions by electrospray ionization tandem mass spectrometry. *J. Mass Spectrom.* **44**, 1224–1233 (2009)
- Cai, Y., Mo, Z., Rannulu, N.S., Guan, B., Kannupal, S., Gibb, B.C., Cole, R.B.: Characterization of an exception to the ‘even-electron rule’ upon low-energy collision induced decomposition in negative ion electrospray tandem mass spectrometry. *J. Mass Spectrom.* **45**, 235–240 (2010)
- Bajpai, L., Varshney, M., Seubert, C.N., Stevens, S.M., Johnson, J.V., Yost, R.A., Dennis, D.M.: Mass spectral fragmentation of the intravenous anesthetic propofol and structurally related phenols. *J. Am. Soc. Mass Spectrom.* **16**, 814–824 (2005)
- Chen, K., Rannulu, N.S., Cai, Y., Lane, P., Liebl, A.L., Rees, B.B., Corre, C., Challis, G.L., Cole, R.B.: Unusual odd-electron fragments from even-electron protonated prodiginine precursors using positive-ion electrospray tandem mass spectrometry. *J. Am. Soc. Mass Spectrom.* **19**, 1856–1866 (2008)
- Xu, G., Huang, T., Zhang, J., Huang, J.K., Carlson, T., Miao, S.: Investigation of collision-induced dissociations involving odd-electron ion formation under positive electrospray ionization conditions using accurate mass. *Rapid Commun. Mass Spectrom.* **24**, 321–327 (2010)
- Hu, N., Tu, Y.-P., Jiang, K., Pan, Y.: Intramolecular charge transfer in the gas phase: Fragmentation of protonated sulfonamides in mass spectrometry. *J. Org. Chem.* **75**, 4244–4250 (2010)
- Chai, Y., Sun, H., Pan, Y., Sun, C.: N-centered odd-electron ions formation from collision-induced dissociation of electrospray ionization generated even-electron ions: Single electron transfer via ion/neutral complex in the fragmentation of protonated *N,N*-dibenzylpiperazines and protonated *N*-benzylpiperazines. *J. Am. Soc. Mass Spectrom.* **22**, 1526–1533 (2011)
- Hau, J., Stadler, R., Jenny, T.A., Fay, L.B.: Tandem mass spectrometric accurate mass performance of time-of-flight and Fourier transform ion cyclotron resonance mass spectrometry: A case study with pyridine derivatives. *Rapid Commun. Mass Spectrom.* **15**, 1840–1848 (2001)
- Denekamp, C., Tenetov, E., Horev, Y.: Homolytic cleavages in pyridinium ions, an excited state process. *J. Am. Soc. Mass Spectrom.* **14**, 790–801 (2003)
- Butler, M., Mañez, P.A., Cabrera, G.M.: An experimental and computational study on the dissociation behavior of hydroxypyridine *N*-oxides in atmospheric pressure ionization mass spectrometry. *J. Mass Spectrom.* **45**, 536–544 (2010)
- Vessecchi, R., Emery, F.S., Galembeck, S.E., Lopes, N.P.: Fragmentation studies and electrospray ionization mass spectrometry of lapachol: Protonated, deprotonated and cationized species. *Rapid Commun. Mass Spectrom.* **24**, 2101–2108 (2010)
- Cuyckens, F., Claeys, M.: Mass spectrometry in the structural analysis of flavonoids. *J. Mass Spectrom.* **39**, 1–15 (2004)
- Cheng, C.-R., Yang, M., Wu, Z.-Y., Wang, Y., Zeng, F., Wu, W.-Y., Guan, S.-H., Guo, D.-A.: Fragmentation pathways of oxygenated tetracyclic triterpenoids and their application in the qualitative analysis of *Ganoderma lucidum* by multistage tandem mass spectrometry. *Rapid Commun. Mass Spectrom.* **25**, 1323–1335 (2011)
- Zhao, Z., Moghadasian, M.H.: Chemistry, natural sources, dietary intake, and pharmacokinetic properties of ferulic acid: A review. *Food Chem.* **109**, 691–702 (2008)
- Itagaki, S., Kurokawa, T., Nakata, C., Saito, Y., Oikawa, S., Kobayashi, M., Hirano, T., Iseki, K.: In vitro and in vivo antioxidant properties of ferulic acid: a comparative study with other natural oxidation inhibitors. *Food Chem.* **114**, 466–471 (2009)
- Barone, E., Calabrese, V., Mancuso, C.: Ferulic acid and its therapeutic potential as a hormetin for age-related diseases. *Biogerontology* **10**, 97–108 (2009)
- Frisch, M.J., Trucks, G.W., Schlegel, H.B., Scuseria, G.E., Robb, M.A., Cheeseman, J.R., Zakrzewski, V.G., Montgomery Jr., J.A., Stratmann, R.E., Burant, J.C., Dapprich, S., Millam, J.M., Daniels, A.D., Kudin, K.N., Strain, M.C., Farkas, O., Tomasi, J., Barone, V., Cossi, M., Cammi, R., Mennucci, B., Pomelli, C., Adamo, C., Clifford, S., Ochterski, J., Petersson, G.A., Ayala, P.Y., Cui, Q., Morokuma, K., Malick, D.K., Rabuck, A.D., Raghavachari, K., Foresman, J.B., Cioslowski, J., Ortiz, J.V., Stefanov, B.B., Liu, G., Liashenko, A., Piskorz, P., Komaromi, I., Gomperts, R., Martin, R.L., Fox, D.J., Keith, T., Al-Laham, M.A., Peng, C.Y., Nanayakkara, A., Gonzalez, C., Challacombe, M., Gill, P.M.W., Johnson, B., Chen, W., Wong, M.W., Andres, J.L., Gonzalez, C., Head-Gordon, M.E., Replogle, S., Pople, J.A.: Gaussian 03. Gaussian Inc., Pittsburgh, PA (2003)
- Tain, Z., Wang, X.-B., Wang, L.-S., Kass, S.R.: Are carboxyl groups the most acidic sites in amino acids? Gas-phase Acidities, photoelectron spectra, and computations on tyrosine, p-hydroxybenzoic acid, and their conjugate bases. *J. Am. Chem. Soc.* **131**, 1174–1181 (2009)
- Steill, J.D., Oomens, J.: Gas-phase deprotonation of p-hydroxybenzoic acid investigated by IR spectroscopy: Solution-phase structure is retained upon ESI. *J. Am. Chem. Soc.* **131**, 13570–13571 (2009)
- Nguyen, M.T., Creve, S., Ha, T.K.: On the formation of the  $\text{CH}_2\text{CH}_2\text{CH} = \text{NH}_2^+$  distonic radical cation upon ionization of cyclopropylamine and allylamine. *Chem. Phys. Lett.* **293**, 90–96 (1998)